JACS
JOURNAL OF THE AMERICAN CHEMICAL SOCIETY
Article
pubs.acs.org/JACS

How a Kinase Inhibitor Withstands Gatekeeper Residue Mutations

Jagannath Mondal,*[,†] Pratyush Tiwary,[‡] and B. J. Berne*[,‡]

[†]Tata Institute of Fundamental Research, Center for Interdisciplinary Sciences, Hyderabad, India
[‡]Department of Chemistry, Columbia University, New York, New York 10027, United States

Supporting Information

ABSTRACT: Mutations in the gatekeeper residue of kinases have emerged as a key way through which cancer cells develop resistance to treatment. As such, the design of gatekeeper mutation resistant kinase inhibitors is a crucial way forward in increasing the efficacy of a broad range of anticancer drugs. In this work we use atomistic simulations to provide detailed thermodynamic and structural insight into how two inhibitors of cSrc kinase, namely, a commercial drug and type I kinase inhibitor Dasatinib and the type II inhibitor RL45, respectively fail and succeed in being effective against the T338M gatekeeper residue mutation in the kinase binding site. Given the well-known limitations of atomistic simulations in sampling biomolecular systems, we use an enhanced sampling technique called free energy perturbation with replica exchange solute tempering (FEP/REST). Our calculations find that the type I inhibitor Dasatinib binds favorably to the wild type but unfavorably to T338M mutated kinase, while RL45 binds favorably to both. The predicted relative binding free energies are well within 1 kcal/mol accuracy compared to experiments. We find that Dasatinib's impotency against gatekeeper residue mutations arises from a loss of ligand−kinase hydrogen bonding due to T338M mutation and from steric hindrance due to the presence of an inflexible phenyl ring close to the ligand. On the other hand, in the type II binding RL45, the central phenyl ring has very pronounced flexibility. This leads to the inhibitor overcoming effects of steric clashes on mutation and maintaining an electrostatically favorable "edge-to-face" orientation with a neighboring phenylalanine residue. Our work provides useful insight into the mechanisms of mutation resistant kinase inhibitors and demonstrates the usefulness of enhanced sampling techniques in computational drug design.

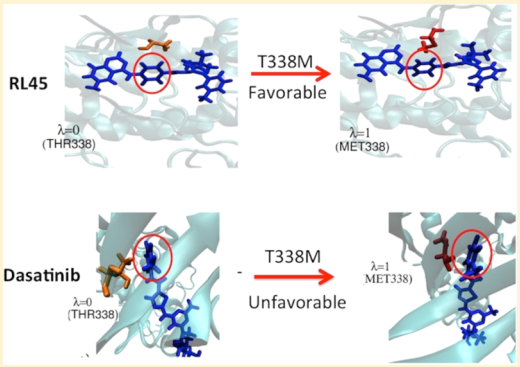

INTRODUCTION

While adenosine triphosphate (ATP) is the cell's energy currency, kinases are the agents controlling the transfer of energy and regulating most aspects of cell life. Abnormal kinase activity correlates with several diseases[1] and can have a significant effect on the dynamics of kinase-associated signaling pathways, ultimately resulting in total cellular deregulation. On the basis of an improved understanding of kinase malfunction in cancer biology, small organic molecule kinase inhibitors have been developed for targeted cancer therapy. These targeted protein−tyrosine kinase inhibitors represent a major advance in cancer treatment.[2,3]

Protein kinases are defined by their ability to catalyze the transfer of the terminal phosphate of ATP to substrates that usually contain a serine, threonine, or tyrosine residue. They typically share a conserved arrangement of secondary structure elements, including a conserved activation loop, which is important in regulating kinase activity and is marked by conserved aspartic acid−phenylalinine−glycine (DFG) motif at the end of the loop.[4,5] Although more than a dozen kinase inhibitors are on the market and are Food and Drug Administration (FDA)-approved, with several more in clinical trials, the onset of drug resistance remains a fundamental challenge in the development of kinase inhibitors.[6] While there are a variety of sources causing drug resistance, in a significant fraction of cases resistance can be traced to mutations in the targeted kinase.[7] The most common mutations occur at the gatekeeper residue in the hinge region of the kinase, and these directly prevent or weaken the interaction with the inhibitor.[8] This can be attributed to the fact that most kinase inhibitors are ATP-competitive molecules, called type I inhibitors.[2,7] In the most typical of these mutations, a relatively smaller amino acid side chain such as threonine (Thr) is exchanged for a larger hydrophobic residue such as methionine (Met) or isoleucine (Ile). Many type I kinase inhibitors such as Dasatinib have been found to be ineffective against the commonly found mutation of Thr to Met at the 338th residue in cSrc and Abl kinases (the so-called T338M mutation).[8−12]

The vulnerability of type I kinase inhibitors to mutations has led to the development of type II kinase inhibitors, which not only bind in the ATP pocket of kinases but also extend past the gatekeeper residue into a less conserved adjacent allosteric site.[7,13] This site is however present exclusively in inactive kinase conformations, which are known as "DFG-out" conformations since the presence of the site is dependent on

Received: February 2, 2016
Published: March 8, 2016

DOI: 10.1021/jacs.6b01232

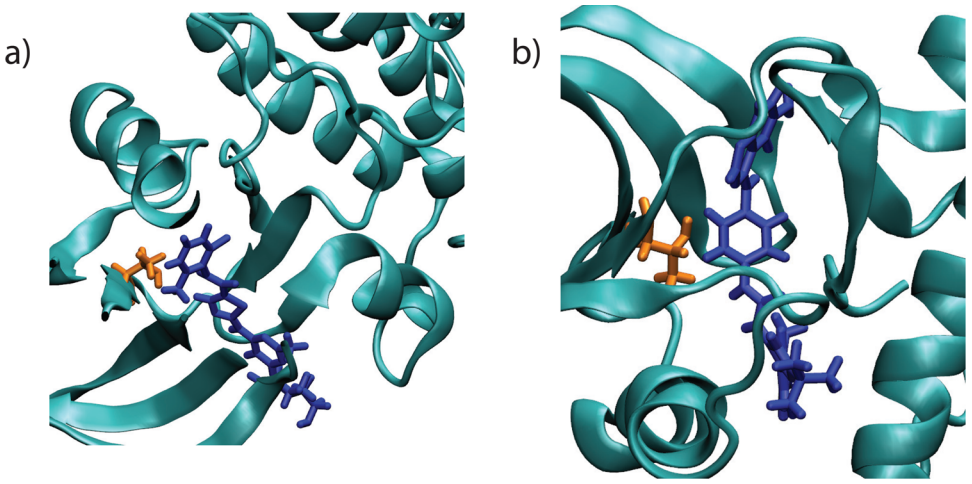

Figure 1. Representative snapshots of ligand (blue color in licorice representation) bound to kinase (cyan color in secondary structure representation) in its native binding pose for (a) Dasatinib−kinase system and (b) RL45−kinase system. Also shown is the gatekeeper residue Thr338 (orange color in licorice representation) which was subjected to mutation in both the ligand−kinase cases.

a significant displacement of the loop comprising the DFG motif. The evidence so far suggests that type II inhibitors can be effective even if the kinase has undergone gatekeeper residue mutations.[8,14] However, a clear mechanistic understanding has remained elusive as to why a type II inhibitor, as contrasted to a type I inhibitor, can be agnostic to gatekeeper residue mutations in the kinase.[2]

In the current work to develop such an understanding, we use an enhanced sampling method called free energy perturbation with replica exchange solute tempering (FEP/REST).[15] Among the various computational methods to calculate protein−ligand binding affinities, free energy perturbation (FEP) calculations[16] performed in explicit solvent are expected to provide a thermodynamically complete description of binding and maximally accurate predictions within the limits of the classical force field used. However, adequate sampling of all of the relevant conformations and converging the free energy calculations within 0.5−1 kcal/mol uncertainty with FEP has been very difficult when high barriers separate some of the stable conformations. In this respect, FEP/REST, a recently developed enhanced sampling technique, is emerging as an excellent alternative to regular FEP calculations.[17,18]

In the current work, we perform fully atomistic molecular dynamics simulations in explicit water with sampling enhanced through FEP/REST, in order to gain insight into the behavior of two kinase inhibitors toward cSrc-kinase, with and without T338M gatekeeper residue mutation (see Figure 1). Specifically, by estimation of relative binding affinities, we show that Dasatinib, an FDA-approved type I kinase inhibitor,[8] loses its binding efficacy upon gatekeeper residue mutation in the kinase. In agreement with experimental results, our calculations find that the type II kinase inhibitor RL45[8] can circumvent the same T338M gatekeeper residue mutation and maintain potency against both the wild type and the mutated kinase. The computed relative binding free energy via the FEP/REST technique is found to be accurate within 0.5−1 kcal/mol uncertainty. Finally, we delve into the details of the structural and mechanistic understanding of Dasatinib's failure and RL45's success to get around the gatekeeper residue mutation, and quantitatively correlate the flexibility of the ligands with success or failure in eventual binding.

SIMULATION MODEL AND METHOD

Conventional FEP[19−21] involves computing the free energy difference between two systems by gradually perturbing from one to the other in a series of discrete steps, represented by λ values, where λ varies from 0 for the initial state to 1 for the final state. FEP/REST significantly enhances the computational efficiency of this process and allows accurate sampling of stable states separated by high barriers. To do so, FEP/REST[15] modifies the underlying potential energy for a localized region comprising protein, ligand, and solvent in the vicinity of the binding pocket, which we call the "hot" region. For the intermediate λ windows, the potential energy for the hot region is scaled by a factor less than 1. In this way, energy barriers are lowered, enabling efficient sampling of the different conformations in these intermediate λ windows, which are then propagated to the end states through the Hamiltonian replica exchange method that satisfies the principle of detailed balance. As has been pointed out in recent studies,[17,18] FEP/REST simulations provide a promising direction for computation of highly accurate relative binding free energies.

The starting configurations for the type I inhibitor Dasatinib and type II inhibitor RL45 bound to cSrc kinase in its wild type form (i.e., Thr as the 338th residue) were taken from the crystallography database (PDB id's 3G5D and 3F3V, respectively).[8] The central goal of the study was to compute the changes in the free energy of binding of both ligands to protein due to mutation of the gatekeeper residue Thr338 to Met338. Both the initial configurations were processed using Protein Preparation Wizard software,[22] in which the protonation states were assigned assuming a pH of 7.0. The systems were solvated in a water box with buffer width of 5 Å, and counterions were added to ensure electroneutrality of the system. The OPLS 2.1 force field was used for the protein and ligand,[23] and the TIP4P water model[24] was used for the water. Figure 1 illustrates representative snapshots of the respective ligands (a) Dasatinib and (b) RL45 bound to the protein in its wild type form. The gate keeper residue Thr338, which is central to our study, is also highlighted to show its relative proximity to the respective ligand.

All simulations were performed using Schrodinger Inc.'s Maestro software package.[25] As is routine for any free energy perturbation method, two separate systems were simulated: one

where the protein bound to ligand undergoes the mutation T338M (the so-called "protein-in-complex" state with the corresponding free energy change referred to as $\Delta G_{complex}$) and the other where the ligand-free protein undergoes the same mutation (so-called "protein-in-solvent" state and corresponding free energy change referred as $\Delta G_{protein}$). In each case, the system was relaxed and equilibrated using the default Desmond[26] relaxation protocol implemented within the multisim utility of Maestro. The difference in binding free energy for the binding of the ligand to the wild type versus the mutant is then

$$\Delta\Delta G = \Delta G_{complex} - \Delta G_{protein}$$

To prepare each system for simulation, the solute molecules were constrained to their initial positions and the energy was minimized. The system was then simulated at 10 K first in the NVT ensemble followed by in the NPT ensemble and subsequently at room temperature in the NPT ensemble. Finally, with the constraints removed, the system was simulated at room temperature in the NPT ensemble for 240 ps followed by the production simulation.

The FEP simulation was carried out in discrete steps for a series of coupling parameters λ with values ranging from $\lambda = 0$ (corresponding to the protein with Thr338) to $\lambda = 1$ (corresponding to the protein with Met338). In this work, we use the heavy atoms of the 338th residue of the protein (the location of mutation) to define the hot region described in the beginning of this section. We use a total of 12 λ windows for the FEP/REST simulations with the effective temperature profiles 300, 410, 547, 717, 931, 1200, 1200, 931, 717, 547, 410, and 300 K, ensuring the same (300 K) temperature for $\lambda = 0.0$ and $\lambda = 1.0$. Each λ window was sampled for 5 ns for both the complex and solvent simulations using NPT ensemble conditions. During FEP/REST simulations, replica exchanges between neighboring λ windows were attempted every 1.2 ps. The Bennett acceptance ratio method (BAR)[27] was used to calculate the free energy. In order to quantitatively compare the performance of the FEP/REST protocol versus the conventional FEP protocol, we also carried out a FEP simulation at 300 K using an identical number of replicas.

RESULTS AND DISCUSSION

A widely used metric for determining the relative binding affinity of a ligand to a wild-type protein and to a mutant is the ratio of IC50 values of the two proteins. IC50 is defined as the half maximal inhibitory concentration of the ligand and is a measure of the effectiveness of a substance in inhibiting a specific biological or biochemical function. As such, the traditional method of quantifying the effect of a mutation is through this ratio. The relative free energy of binding (as discussed in detail in the Supporting Information) was given by Cheng and Prussoff,[28] who showed that when a group of inhibitory compounds have a similar type of action on the target, the ratio of IC50 will be effectively the same as the ratio of binding constants of the ligand (see Supporting Information text for details).

$$\Delta\Delta G = \Delta G_{mutant} - \Delta G_{wild\text{-}type} \sim RT \ln\left[\frac{(IC50)_{wild\text{-}type}}{(IC50)_{mutant}}\right] \quad (1)$$

where $T = 300$ K, R is the gas constant, and the subscripts denote respective proteins. Equation 1 has been utilized quite successfully in numerous studies[17,29−31] to determine an estimate of the relative free energy of binding from IC50 data, in lieu of ligand binding constant data. It was also shown that this equation is valid when the substrate concentration is much lower than the Michelis−Menten constant. The reported experimental assay by Getlik et al.[8] showed that the conditions required for the eq 1 to be valid were met for both wild-type and T338M-mutated kinase (see Supporting Information). Under such a condition, the ligand binding constant becomes effectively equal to IC50, as is the case in the present work.

In Table 1, we compare $\Delta\Delta G$ values from our simulations versus known benchmarks from experiments.[8] For Dasatinib,

Table 1. Predicted Relative Binding Free Energies (in kcal/mol) of the Ligand to Kinase Due to T338M Mutation at the Gatekeeper Residue

system	method	$\Delta G_{complex}$	$\Delta G_{protein}$	$\Delta\Delta G$
Dasatinib/kinase				
	FEP	10.34	1.65	8.70
	FEP/REST	6.97	2.40	4.57
	experiment			4.26
RL45/kinase				
	FEP	0.75	6.40	−5.65
	FEP/REST	1.76	2.84	−1.08
	experiment			0.30

FEP/REST simulations find an unfavorable change in free energy following mutation of the gatekeeper residue from Thr338 to Met338, in excellent quantitative agreement with experiment, indicating that a T338M mutation in the kinase will render a type I drug like Dasatinib ineffective. On the other hand, FEP/REST simulations find that the type II inhibitor RL45 can withstand a T338M mutation, with a slightly favorable free energy change upon mutation. This result is also in near-quantitative agreement with experimental observations, suggesting that the binding of ligand RL45 can withstand the gatekeeper mutation. Note that the experimental value of $\Delta\Delta G$ for RL45 is nearly zero, suggesting that at room temperature the binding affinity of RL45 to both wild-type and mutated kinases is essentially the same. On the other hand, the FEP/REST estimate of $\Delta\Delta G = 1$ kcal/mol suggests that that RL45 binds very slightly more strongly to the mutated kinase; however the difference between experiment and simulation for $\Delta\Delta G$ is well within thermal fluctuations and is insignificant considering force-field errors and the non-negligible uncertainty of 0.034 ± 0.012 mM in the experimental IC50 value of RL45 binding to T338M-mutated kinase.

In contrast with FEP/REST, FEP alone drastically overestimates the effect of the mutation on the binding of Dasatinib or RL45 to kinase, leading to qualitatively incorrect results. Our results clearly establish that the FEP/REST method with its significantly enhanced sampling efficiency over FEP has the predictive power to treat the effect of mutations on the binding affinities of ligands to kinase and is in near-quantitative agreement with experiment.

We now seek an atomic level understanding of why the type I inhibitor Dasatinib becomes ineffective against the T338M mutation, while the type II inhibitor RL45 retains its binding potency. For this we perform a detailed analysis of the FEP/REST simulation trajectories at $\lambda = 0.0$ (kinase in wild-type form with Thr in 338th residue) and $\lambda = 1.0$ (kinase in mutated form with Met in 338th residue).

DOI: 10.1021/acs.jcim.6b01333

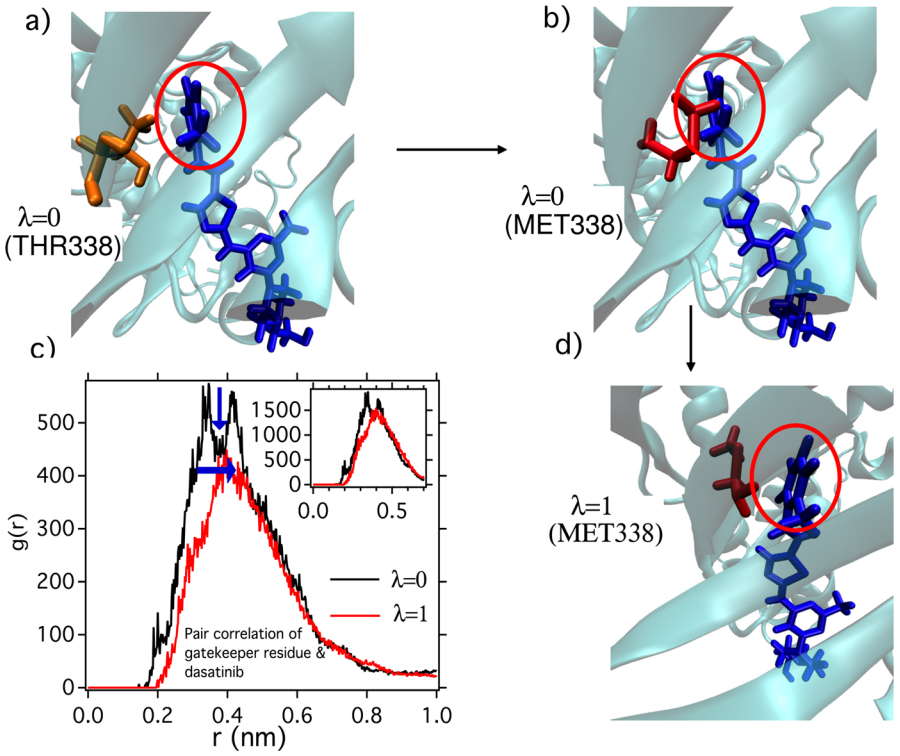

Figure 2. Representative snapshots of Dasatinib (blue licorice) interacting with the gatekeeper residue (orange color) of the host kinase at various stages of FEP/REST simulation. The phenyl ring of Dasatinib proximal to the gatekeeper residue has been highlighted by red circle. (a) At $\lambda = 0.0$ the gatekeeper residue is in its wild-type stage Thr338, and it interacts favorably with Dasatinib. (b) At $\lambda = 0.0$, attempts to alchemically mutate Thr338 to Met338 becomes sterically hindered. (d) At $\lambda = 1.0$, in the fully mutated stage Met338 moves away from Dasatinib to avoid steric overlap. (c) Comparison of pair correlation of gate keeper residue with Dasatinib at wild-type ($\lambda = 0.0$) and mutated stage ($\lambda = 1.0$). The major peak in the correlation curve becomes less intense and at a relatively higher separation on morphing from Thr338 to Met338, in order to avoid steric overlap with the ligand. Inset: the pair correlation of gatekeeper residue with the proximal phenyl ring of the Dasatinib. The directional horizontal and vertical arrow in (c) signifies the drop in peak intensity and shift toward larger distance on morphing of Thr338 to Met338.

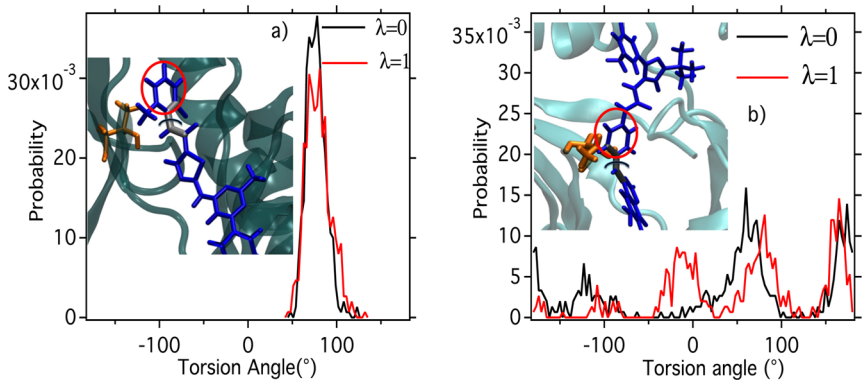

Figure 3. Quantification of flexibility of phenyl ring of the ligand proximal to the gatekeeper residue studied using FEP/REST: (a) The distribution of the torsional angle of the phenyl ring of Dasatinib at $\lambda = 0.0$ (wild-type) and $\lambda = 1.0$ (mutated) stage. The narrow distribution of the phenyl ring's torsion angle indicates the phenyl ring's lack of flexibility. (b) The distribution of the torsional angle of the phenyl ring of RL45 for $\lambda = 0.0$ (wild-type) and $\lambda = 1.0$ (mutant). Its wide distribution in both the wild-type and mutant quantifies the high flexibility of the phenyl ring in RL45 that helps it to withstand the gatekeeper residue mutation.

Insights into How Dasatinib Becomes Ineffective upon T338M Mutation of Gatekeeper Residue. As depicted in Figure 2, representative snapshots from our Dasatinib–kinase FEP/REST trajectories reveal that an attempt to morph Thr to Met at the 338th residue imparts a potentially significant steric strain to Dasatinib. This is due to the overlap between the methyl side chain of Met and the proximal phenyl ring of Dasatinib. Consequently, in the mutated kinase, Met338 moves away from Dasatinib to avoid the steric overlap. This result is further validated by a comparison of the pair correlation functions of the gatekeeper residue and Dasatinib. As shown in Figure 2c, upon mutation of T338M in the gatekeeper residue, the most prominent peak in the pair correlation function gets shifted to relatively larger distances, and the peak intensity as well drops significantly, resulting in reduced protein–ligand interaction upon mutation. A detailed analysis of the distribution of torsional angles of the phenyl ring of Dasatinib adjacent to the gatekeeper residue further clarifies

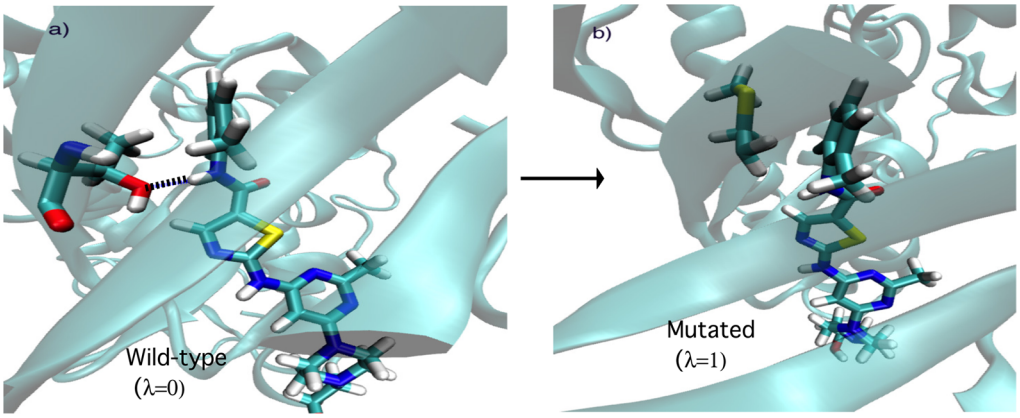

Figure 4. (a) Representative snapshot of gatekeeper residue (Thr338) hydrogen bonding (shown by thick black line) with Dasatinib in the wild-type (λ = 0.0) system. (b) Mutation of gatekeeper residue to met338 (λ = 1.0) disrupts the hydrogen bond formation with Dasatinib.

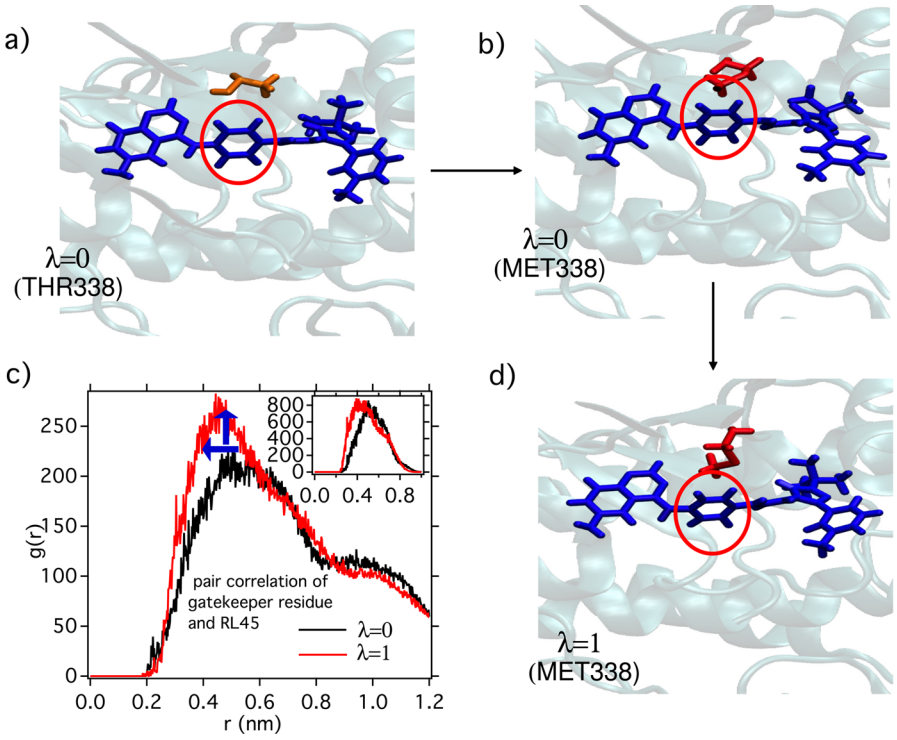

Figure 5. Representative snapshots of RL45 (blue licorice) interacting with the gatekeeper residue (orange color) of the host kinase at various stages of FEP/REST simulation. The phenyl ring of RL45 proximal to the gatekeeper residue has been highlighted by red circle. (a) At λ = 0.0 the gatekeeper residue is in its wild-type stage Thr338, and it interacts favorably with the Dasatinib. (b) At λ = 0.0, attempts to alchemically mutate Thr338 to Met338 is still favorable, and no steric interaction is encountered. (d) At λ = 1.0, in the fully mutated stage Met338 interacts favorably with RL45 due to high flexibility of the proximal phenyl ring (see Figure 3b). (c) Comparison of pair correlation of gate keeper residue with Dasatinib at wild-type (λ = 0.0) and mutated stage (λ = 1.0). In contrast to Dasatinib (Figure 2c), the major peak in the correlation curve now becomes slightly more intense and at a relatively smaller separation on morphing from Thr338 to Met338 because the Met338 side chain can dangle further due to the flexibility of proximal phenyl ring of RL45. Inset: the pair correlation of gatekeeper residue with the proximal phenyl ring of the RL45. The directional horizontal and vertical arrows in (c) signify the increase in peak intensity and shift toward shorter distance on morphing of Thr338 to Met338.

the role of this ring. As illustrated in Movie 1 in the Supporting Information, it is its lack of flexibility that prevents the ligand from circumventing the impending steric strain caused by bulky side chains of Met338. As illustrated by the narrow distribution of torsional angles in Figure 3a, the conformational rigidity of the phenyl ring of Dasatinib adds to its ineffectiveness in adapting to the T338M mutation of the gatekeeper residue.

We also find that the hydroxyl side chain of the wild-type gatekeeper residue Thr338 makes a stable hydrogen bond with Dasatinib. However, as shown in Figure 4, we find that the mutation of the gatekeeper residue from Thr (with its hydroxyl side chain) to Met (with its methyl side chain) disrupts the hydrogen bond between the gatekeeper residue and Dasatinib and reduces the Dasatinib−kinase binding propensity significantly. Taken together, we believe that the inflexibility of the phenyl ring to avoid the steric strain of the mutated residue, coupled with the disruption of a key hydrogen bond upon

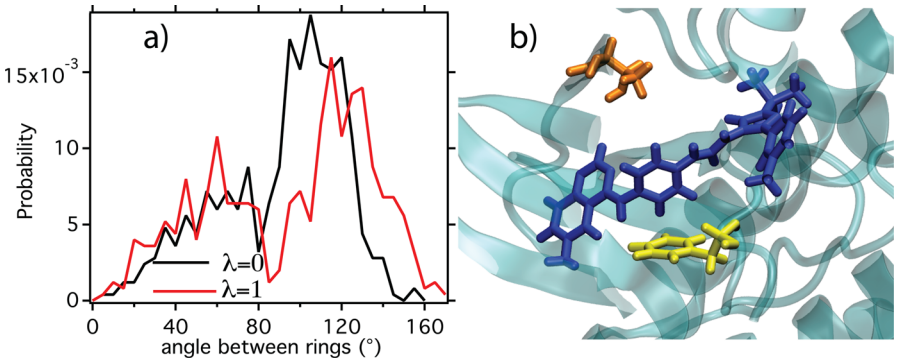

Figure 6. (a) Distribution of the angle between planes of the central phenyl ring of RL45 and the phenyl rings of F405 of kinase. The distribution is predominantly peaked at an angle of 90°, suggesting the persistence of highly electrostatically favorable "edge-to-face" orientation of two phenyl rings in both $\lambda = 0.0$ and $\lambda = 1.0$ (b) A representative snapshot of "edge-to-face" orientation of two phenyl rings. The phenyl ring of Phe405 is colored yellow while other colors are in the same scheme as previous Figures.

mutation, renders Dasatinib ineffective against a T338M gatekeeper residue mutation.

Insights into How RL45 Retains Its Effectiveness upon T338M Mutation. The FEP/REST calculations show that the type II inhibitor RL45 remains bound under the T338M mutation. Simulations show that this is mainly due to the remarkable flexibility of the ligand phenyl ring proximal to the location of the mutation as illustrated in Figure 3b, where the distribution of the phenyl ring torsion angles of RL45 proximal to the gatekeeper residue is very broadly spread. Unlike what happens in Dasatinib, the phenyl ring in RL45 is flexible enough to avoid any potential steric strain due to mutation of Thr338 to Met338. This is corroborated by the representative snapshots in Figure 5.

As shown in Figure 5a,b,d, attempts to morph the side chain of Thr338 to that of Met338 are easily accommodated by RL45 as the central phenyl ring spins around its axis to avoid any steric overlap (illustrated in Movie 2 in Supporting Information). In fact, as quantified by the RL45−gatekeeper residue pair correlation function, the major peak becomes more intense and shifts toward smaller separations in the mutated protein. This is mainly because the dangling side chain of Met338 can reach out further toward the phenyl ring of the RL45, then can the shorter side chain of Thr338, and this leads to more favorable interactions with the ligand.

A careful inspection of the trajectories (see Movie 3 in Supporting Information) in both wild-type and mutated forms reveals persistent occurrence of an interesting "edge-to-face" orientation of the central phenyl ring of RL45 relative to the phenyl ring of Phe405, which is a part of the DFG motif (see Figure 6b). This "edge-to-face" orientation of two phenyl rings is well-known for its high electrostatic stability.[32] As quantified by the distributions of the angles between the planes of the two phenyl rings in Figure 6a, the orientation is predominantly peaked around 90°in both the wild-type and the mutated forms. We believe that the ability to maintain the near-perpendicular orientation of phenyl rings in both wild-type and mutated forms, and hence the similar binding affinity is mainly due to the high flexibility of the central phenyl ring of RL45.

We also find that the ligand−protein hydrogen bond distributions in RL45 (see Supporting Information Figure S1) do not alter upon mutation of the gatekeeper residue unlike in Dasatinib. Finally, the excellent overlay (Figure S2) of the simulated ligand-binding pose of RL45 in the mutant kinase with the corresponding crystallographic structure (PDB id: 3F3W) speaks highly in favor of the FEP/REST method.

CONCLUSIONS

In this paper we have used FEP/REST, an enhanced sampling based free energy simulation method, to gain mechanistic and structural insights into how a type I kinase inhibitor Dasatinib fails to cope with a single-point-mutation (T338M) of the gatekeeper residue in cSrc kinase, while a type II kinase inhibitor RL45 binds with the mutated gatekeeper residue effectively as strongly as with the wild type. The computed relative ligand-binding free energy upon mutation is accurate within 0.5−1 kcal/mol compared to experiments. Our analysis shows that the relative lack of flexibility of Dasatinib prevents it from avoiding steric clashes, an effect that weakens its binding to the mutant. Moreover, it also loses a crucial ligand−pocket hydrogen bond when the protein is mutated further reducing its binding affinity to the mutated kinase. On the other hand, our simulations suggest a mechanistic rationale for why the type II kinase inhibitor RL45 is able to withstand the gatekeeper residue mutation. We find that it is the significant flexibility of the central phenyl ring of RL45 which enables it to bind to the mutant without any loss of the ligand−protein hydrogen bonding network. In view of the detailed understanding that we could achieve through FEP/REST, we believe this method can be useful not only in providing key mechanistic insights for the action of kinase inhibitors but also for high-throughput screening and for designing new series of potent kinase inhibitors.

The computer simulations in this paper provide detailed structural and pictorial insights into how a gatekeeper residue mutation of the kinase renders some previously effective ligands ineffective as drugs, whereas other ligands remain effective. The sampling schemes employed in this work do not stop at just reproducing the relative binding free energies of the wild-type and the mutant kinase but also show how ligand flexibility plays a role in binding by exploring the torsional phase space and confirms certain previous ideas. Computer simulations in which the whole system is dynamically propagated explore fluctuations which play an exceedingly important role and fill an elusive gap between static crystal poses determined from X-ray crystallography and thus allow one to validate or invalidate models and hypotheses based on, but not proved, by laboratory experiments. Whereas the structures of ligands bound to proteins determined by X-ray crystallography are a major

source of information, it is important to remember that such methods often give only a static picture of the system in its native pose rather than the ensemble of structures often obtained from enhanced sampling computer simulations.

This paper does not make a generic statement that type II inhibitors are almost always more potent than type I inhibitors. We believe that performance against gatekeeper residue mutation has to be judged on a case-by-case basis, rather than on the classification as type I or type II kinase inhibitors. Our work focuses on a specific type II ligand namely RL45 as synthesized by Getlik et al.,[8] which has been experimentally found to circumvent the gatekeeper residue mutation (unlike a type I drug namely Dasatinib), and our computational results are consistent with this experimental observation. In fact, Dasatinib has a larger absolute binding affinity to the wild-type kinase than does RL45, whereas the inhibitor RL45 has a larger binding affinity to the gatekeeper mutant than does Dasatinib. This should be compared to Imatinib, the founding type II inihibitor, which is inactive against the gatekeeper residue mutation. But we also note that there are numerous instances where type II inhibitors have been effective against gatekeeper residue mutation. For example, HG-7-85-01, a type II kinase inhibitor, has been reported[33] to be capable of circumventing several gatekeeper residue mutations (T315I in BCR-ABL, T617I in kit), and a new type II drug Ponatinib[34] binds efficiently in the presence of the T315I gatekeeper residue and is 400−500-fold more effective than Imatinib.

One issue that we have not addressed in this work pertains to distinguishing between "induced fit" and "conformational selection" modes of molecular recognition of the kinase.[35,36] While the conformational selection hypothesis proposes the "fold-first" mechanism,[37] the induced-fit hypothesis emphasizes on "bind-first" mechanism.[38] In fact, both the mechanisms might work in tandem. In this regard we would like to point out that an analysis of the thermodynamics of relevant stable states such as ours cannot differentiate conformational selection from induced fit. A clear understanding of conformational selection versus induced fit would require a detailed kinetic analysis[39,40] which we will be performing in the future.

■ ASSOCIATED CONTENT

Supporting Information

The Supporting Information is available free of charge on the ACS Publications website at DOI: 10.1021/jacs.6b01232.

Comparison of distribution of hydrogen bonds between RL45 and kinase in wild-type and mutant, overlay of simulated and crystal data of RL45 bound to mutated kinase, thumbnails of movies 1, 2, and 3 (PDF)

Trajectory showing the inexibility of phenyl ring of Dasatinib to avoid steric overlap upon mutation (AVI)

Trajectory showing the remarkable exibility of central phenyl ring of RL45 in adapting to mutation (AVI)

Trajectory showing the persistence of edge-to-face orientation of central phenyl ring of RL45 with Phe405 (AVI)

■ AUTHOR INFORMATION

Corresponding Authors

*E-mail jmondal@tifrh.res.in (J.M.).

*E-mail bb8@columbia.edu (B.J.B.).

Notes

The authors declare the following competing financial interest(s): B.J.B. is a consultant to Schrodinger, Inc., and is on their Scientific Advisory Board..

■ ACKNOWLEDGMENTS

We thank Anthony Clark for help with Schrodinger's Maestro software package. This work was supported by grants from the National Institutes of Health [NIH-GM4330] and the Extreme Science and Engineering Discovery Environment (XSEDE) [TG-MCA08X002] to B.J.B. J.M. would like to acknowledge financial support from Tata Institute of Fundamental research and DST funding under Ramanujan fellowship program.

■ REFERENCES

(1) Cohen, P. *Nat. Rev. Drug Discovery* **2002**, *1*, 309−15.

(2) Zhang, J.; Yang, P. L.; Gray, N. S. *Nat. Rev. Cancer* **2009**, *9*, 28−39.

(3) Gschwind, A.; Fischer, O. M.; Ullrich, A. *Nat. Rev. Cancer* **2004**, *4*, 361−370.

(4) Treiber, D. K.; Shah, N. P. *Chem. Biol.* **2013**, *20*, 745−746.

(5) Hari, S.; Merritt, E.; Maly, D. *Chem. Biol.* **2013**, *20*, 806−815.

(6) Daub, H.; Specht, K.; Ullrich, A. *Nat. Rev. Drug Discovery* **2004**, *3*, 1001−10.

(7) Bikker, J. A.; Brooijmans, N.; Wissner, A.; Mansour, T. S. *J. Med. Chem.* **2009**, *52*, 1493−1509.

(8) Getlik, M.; Grütter, C.; Simard, J. R.; Klüter, S.; Rabiller, M.; Rode, H. B.; Robubi, A.; Rauh, D. *J. Med. Chem.* **2009**, *52*, 3915−26.

(9) Blencke, S.; Ullrich, A.; Daub, H. *J. Biol. Chem.* **2003**, *278*, 15435−15440.

(10) Carter, T. A.; Wodicka, L.; Shah, N. P.; Velasco, A. M.; Fabian, M. A.; Treiber, D. A.; Milanov, Z. V.; Biggs, W. H.; Edeen, P. T.; Floyd, M.; Ford, J. M.; Grotzfeld, R. M.; Herrgard, S.; Insko, D. E.; Mehta, S. A.; Patel, H. T.; Pao, W.; Sawyers, C. L.; Varmus, P. Z.; Zarrinkar, P. P.; Lockhart, D. J. *Proc. Natl. Acad. Sci. U. S. A.* **2005**, *102*, 11011−11016.

(11) Lovera, S.; Morando, M.; Pucheta-Martinez, E.; Martinez-Torrecuadrada, J. L.; Saladino, G.; Gervasio, F. L. *PLoS Comput. Biol.* **2015**, *11*, e1004578.

(12) Gibbons, D. L.; Pricl, S.; Posocco, P.; Laurini, E.; Fermeglia, M.; Sun, H.; Talpaz, M.; Donato, N.; Quintás-Cardama, A. *Proc. Natl. Acad. Sci. U. S. A.* **2014**, *111*, 3550−3555.

(13) Liu, Y.; Gray, N. S. *Nat. Chem. Biol.* **2006**, *2*, 358−364.

(14) Peng, Y.-h.; Shiao, H.-y.; Tu, C.-h.; Liu, P.-m.; Hsu, J. T.-A.; Wang, S.-y.; Lin, W.-h.; Sun, H.-y.; Chao, Y.-s.; Lyu, P.-c.; Hsieh, H.-p. *J. Med. Chem.* **2013**, *56*, 3889−3903.

(15) Wang, L.; Berne, B. J.; Friesner, R. A. *Proc. Natl. Acad. Sci. U. S. A.* **2012**, *109*, 1937−1942.

(16) Gallicchio, E.; Levy, R. M. *Curr. Opin. Struct. Biol.* **2011**, *21*, 161−166.

(17) Wang, L.; Wu, Y.; Deng, Y.; Kim, B.; Pierce, L.; Krilov, G.; Lupyan, D.; Robinson, S.; Dahlgren, M.; Greenwood, J.; Romero, D.; Masse, C.; Knight, J.; Steinbrecher, T.; Beuming, T.; Damm, W.; Harder, E.; Sherman, W.; Brewer, M.; Wester, R.; Murcko, M.; Frye, L.; Farid, R.; Lin, T.; Mobley, D.; Jorgensen, W. L.; Berne, B. J.; Friesner, R. A.; Abel, R. *J. Am. Chem. Soc.* **2015**, *137*, 2695−2703.

(18) Wang, L.; Deng, Y.; Knight, J. L.; Wu, Y.; Kim, B.; Sherman, W.; Shelley, J. C.; Lin, T.; Abel, R. *J. Chem. Theory Comput.* **2013**, *9*, 1282−1293.

(19) Zwanzig, R. W. *J. Chem. Phys.* **1954**, *22*, 1420−1426.

(20) Chodera, J. D.; Mobley, D. L.; Shirts, M. R.; Dixon, R. W.; Branson, K.; Pande, V. S. *Curr. Opin. Struct. Biol.* **2011**, *21*, 150−160.

(21) Hansen, N.; Van Gunsteren, W. F. *J. Chem. Theory Comput.* **2014**, *10*, 2632−2647.

(22) Madhavi Sastry, G.; Adzhigirey, M.; Day, T.; Annabhimoju, R.; Sherman, W. *J. Comput.-Aided Mol. Des.* **2013**, *27*, 221−234.

(23) Shivakumar, D.; Harder, E.; Damm, W.; Friesner, R. A.; Sherman, W. *J. Chem. Theory Comput.* **2012**, *8*, 2553−2558.
(24) Jorgensen, W. L.; Chandrasekhar, J.; Madura, J. D.; Impey, R. W.; Klein, M. L. *J. Chem. Phys.* **1983**, *79*, 926−935.
(25) Schrödinger suite 2012 Protein Preparation Wizard (Schrödinger, New York). http://www.schrodinger.com, 2012.
(26) SC '06: Proceedings of the 2006 ACM/IEEE Conference on Supercomputing, 2006.
(27) Bennett, C. H. *J. Comput. Phys.* **1976**, *22*, 245−268.
(28) Yung-Chi, C.; Prusoff, W. H. *Biochem. Pharmacol.* **1973**, *22*, 3099−3108.
(29) Price, M. L. P.; Jorgensen, W. L. *J. Am. Chem. Soc.* **2000**, *122*, 9455−9466.
(30) Luccarelli, J.; Michel, J.; Tirado-Rives, J.; Jorgensen, W. L. *J. Chem. Theory Comput.* **2010**, *6*, 3850−3856.
(31) Michel, J.; Verdonk, M. L.; Essex, J. W. *J. Med. Chem.* **2006**, *49*, 7427−7439.
(32) Hunter, C. A.; Singh, J.; Thornton, J. M. *J. Mol. Biol.* **1991**, *218*, 837−846.
(33) Weisberg, E.; et al. *Blood* **2010**, *115*, 4206−4216.
(34) Gibbons, D. L.; Pricl, S.; Kantarjian, H.; Cortes, J.; Quintás-Cardama, A. *Cancer* **2012**, *118*, 293−299.
(35) Gianni, S.; Dogan, J.; Jemth, P. *Biophys. Chem.* **2014**, *189*, 33−39.
(36) Vogt, A. D.; Cera, E. D. *Biochemistry* **2012**, *51*, 5894−5902.
(37) Vogt, A. D.; Pozzi, N.; Chen, Z.; Cera, E. D. *Biophys. Chem.* **2014**, *186*, 13−21. Special issue: conformational selection.
(38) Wilson, C.; Agafonov, R. V.; Hoemberger, M.; Kutter, S.; Zorba, A.; Halpin, J.; Buosi, V.; Otten, R.; Waterman, D.; Theobald, D. L.; Kern, D. *Science* **2015**, *347*, 882−886.
(39) Tiwary, P.; Parrinello, M. *Phys. Rev. Lett.* **2013**, *111*, 230602−230606.
(40) Tiwary, P.; Mondal, J.; Morrone, J. A.; Berne, B. *Proc. Natl. Acad. Sci. U. S. A.* **2015**, *112*, 12015−12019.